

Mass spectra of heavy hybrid quarkonia and $\bar{b}gc$ mesons

A. Alaakol,¹ S. S. Agaev,² K. Azizi,^{3,4,*} and H. Sundu⁵

¹*Department of Physics, Marmara University, 34722 Istanbul, Türkiye*

²*Institute for Physical Problems, Baku State University, Az-1148 Baku, Azerbaijan*

³*Department of Physics, University of Tehran, North Karegar Avenue, Tehran 14395-547, Iran*

⁴*Department of Physics, Doğuş University, Dudullu-Ümraniye, 34775 Istanbul, Türkiye*

⁵*Department of Physics Engineering, Istanbul Medeniyet University, 34700 Istanbul, Türkiye*

(ΩDated: May 17, 2024)

Masses and current couplings of the charmonium and bottomonium hybrids $\bar{c}gc$ and $\bar{b}gb$ with spin-parities $J^{PC} = 0^{++}, 0^{+-}, 0^{-+}, 0^{--}$ and $1^{++}, 1^{+-}, 1^{-+}, 1^{--}$ are calculated using QCD two-point sum rule method. Computations are performed by taking into account gluon condensates up to dimension 12 including terms $\sim \langle g_s^3 G^3 \rangle^2$. The parameters of the bottom-charm hybrids $\bar{b}gc$ with quantum numbers $J^{PC} = 0^+, 0^-, 1^+,$ and 1^- are calculated as well. In computations the dominance of the pole contribution to sum rule results is ensured. It is demonstrated that all charmonia hybrids decay strongly to two-meson final states. The bottomonium hybrids 0^{-+} and 1^{-+} as well as the bottom-charm hybrid mesons $0^{-(+)}$ and $1^{-(+)}$ may be stable against strong two-meson decay modes. Results of the present work are compared with ones obtained using the sum rule and alternative approaches. Our predictions for parameters of the heavy hybrid mesons may be useful to study their various decay channels which are important for interpretation of ongoing and future experiments.

I. INTRODUCTION

It is well known that apart from conventional mesons and baryons, QCD and parton model do not forbid existence of multi-quark states, glueballs, and hybrid structures. Experimental investigations of last years allowed one to collect valuable information about tetraquark and pentaquark candidates. The X resonances presumably composed of four charm quarks (antiquarks) [1–3], and structures $P_c(4330)$, $P_c(4440)$, and $P_{cs}(4459)$ [4–6] discovered recently are among promising candidates to tetra- and pentaquarks, respectively.

Charmonium and bottomonium hybrids, i.e., mesons which besides valence quarks and antiquarks contain also valence gluon(s), as well as bottom-charm hybrids $\bar{b}gc$ belong also to a class of exotic states. There are a few candidates to light hybrid mesons discovered in various experiments. Namely, mesons $\pi_1(1400)$, $\pi_1(1600)$ and $\pi_1(2105)$ are such states. Recently, the BESIII collaboration informed about the isoscalar vector resonance $\eta_1(1855)$ with exotic quantum numbers $J^{PC} = 1^{-+}$ [7], which was observed in the process $J/\psi \rightarrow \gamma \eta_1(1855) \rightarrow \gamma \eta \eta'$. This resonance is considering as possible hybrid meson [8–10] though alternative hadronic molecule and/or diquark-antidiquark models were suggested to explain corresponding experimental data.

There are candidates to hybrid mesons among heavy resonances as well. Thus, it was argued that the vector resonances $\psi(4230)$ and $\psi(4360)$ may be hybrid charmonium states $\bar{c}gc$ or their essential components [11, 12]. Detailed information about numerous resonances that may be considered as candidates to hybrid quarkonia can be found in Ref. [13]. The hybrids with baryon quantum numbers are also among exotic hadrons. The $\Lambda(1405)$ discovered many years ago [14] and investigated by various collaborations as a candidate to such baryon [15–17].

Theoretical studies of hybrid hadrons have long story: Existence of such states was supposed more than four decades ago in Refs. [18, 19]. Interesting results concerning spectroscopic parameters of hypothetical hybrid particles, their decay and production mechanisms were obtained at early stages of investigations in the context of different methods [20–31]. These studies were continued in Refs. [32–52] aimed to refine calculational schemes and methods used in relevant analyses. The hybrid states were explored by means of QCD sum rule (SR) and lattice methods, constituent gluon, flux-tube and nonrelativistic field theory models which form theoretical basis of these investigations.

The wide diversity of obtained results makes relevant problems actual until now. For instance, in Ref. [33] the masses of the vector 1^{--} hybrids $H_c = \bar{c}gc$ and $H_b = \bar{b}gb$ were evaluated by employing SR approach. Calculations were performed with $\langle g_s^3 G^3 \rangle$ accuracy and predictions $m_{H_c} = 4.12 - 4.79$ GeV and $m_{H_b} = 10.24 - 11.15$ GeV were made for the masses of these particles. The masses of the same hybrids were estimated as (3.36 ± 0.15) GeV and (9.70 ± 0.12) GeV in Ref. [36]. The lattice simulations led to the results (4.41 ± 0.02) GeV and (10.95 ± 0.02) GeV

*Corresponding Author

[38, 44]. Analyses carried out in Ref. [43] yielded $\simeq 4.40$ GeV and $\simeq 10.74$ GeV, respectively. Recently, these problems were addressed in the context of the Born-Oppenheimer effective field theory (BOEFT) [51]. The authors found that 1^{--} states have the masses (4.011 ± 0.030) GeV and (10.6902 ± 0.003) GeV, respectively.

The exotic mesons $\bar{b}gc$ were also in the sphere of researches' interests [37, 42]. The bottom-charmonium hybrids with quantum numbers $J^P = 0^+, 0^-, 1^+, 1^-, 2^+, \text{ and } 2^-$ were considered in Ref. [37]. Calculations were carried out using QCD sum rule approach by taking into account dimension six condensates. The masses of these hybrids were predicted in the range of 6.8 to 8.5 GeV. The authors analyzed their possible strong decays including open- and hidden-flavor two-body exclusive channels. In Ref. [42] the mass spectra and decays of the states $\bar{b}gc$ with magnetic and electric gluon were investigated by means of the constituent gluon model.

In the present article, we compute the masses and current couplings of hybrid quarkonia $\bar{c}gc$ and $\bar{b}gb$, and exotic mesons $\bar{b}gc$ with different spin-parities. Our investigations are performed in the context of QCD two-point SR method by taking into account nonperturbative terms proportional to $\langle g_s^3 G^3 \rangle^2$. The sum rule method is one of effective and powerful nonperturbative tools in high energy physics. It was elaborated to study features of conventional hadrons, and analyze their decay channels [53, 54]. But this approach can be employed to investigate exotic hadrons as well [55–57]. It is remarkable that QCD SRs was successfully applied to investigate the hybrid quarkonia starting from first years of its invention [24–26].

This paper is structured in the following way. In Sec. II, we calculate spectral parameters of the heavy hybrids $\bar{c}gc$ and $\bar{b}gb$ with spin-parities $J^{PC} = 0^{++}, 0^{+-}, 0^{-+}, 0^{--}$ and $1^{++}, 1^{+-}, 1^{-+}, 1^{--}$. Section III is devoted to analysis of the hybrid mesons $\bar{b}gc$ with quantum numbers $J^P = 0^+, 0^-, 1^+, \text{ and } 1^-$. The last section contains our short conclusions.

II. MASS AND CURRENT COUPLING OF THE HEAVY HYBRID QUARKONIA

The sum rules for parameters of the heavy hybrid states $H^c = \bar{c}gc$ and $H^b = \bar{b}gb$ can be extracted from analysis of the correlation function

$$\Pi_{\mu\nu}(p) = i \int d^4x e^{ipx} \langle 0 | \mathcal{T} \{ J_\mu(x) J_\nu^\dagger(0) \} | 0 \rangle. \quad (1)$$

Here $J_\mu(x)$ is the interpolating current for the particle under consideration, and \mathcal{T} stands for a time-ordering product of two currents.

For the scalar and vector hybrids with the negative C-parity $J^{PC} = 0^{+-}$ and 1^{--} the interpolating current has the following form

$$J_\mu^1(x) = g_s \bar{Q}_a(x) \gamma^\alpha \gamma_5 \frac{\lambda_{ab}^n}{2} \tilde{G}_{\mu\alpha}^n(x) Q_b(x), \quad (2)$$

whereas for the particles with the positive C-parity 0^{++} and 1^{+-} it is given by the expression

$$J_\mu^2(x) = g_s \bar{Q}_a(x) \gamma^\alpha \frac{\lambda_{ab}^n}{2} G_{\mu\alpha}^n(x) Q_b(x). \quad (3)$$

In Eqs. (2) and (3), the heavy quark field $Q(x)$ labels c or b quarks. Here g_s is the QCD strong coupling constant, a and b are color indices and λ^n , $n = 1, 2, \dots, 8$ are Gell-Mann matrices. The gluon field strength and its dual tensors are shown by $G_{\mu\nu}^n(x)$ and $\tilde{G}_{\mu\nu}^n(x) = \varepsilon_{\mu\nu\alpha\beta} G^{\alpha\beta}(x)/2$, respectively.

Interpolating currents for the pseudoscalar and axial-vector hybrids are defined by the formulas

$$J_\mu^3(x) = g_s \bar{Q}_a(x) \gamma^\alpha \gamma_5 \frac{\lambda_{ab}^n}{2} G_{\mu\alpha}^n(x) Q_b(x), \quad (4)$$

in the case of the states 0^{--} , 1^{+-} and

$$J_\mu^4(x) = g_s \bar{Q}_a(x) \gamma^\alpha \frac{\lambda_{ab}^n}{2} \tilde{G}_{\mu\alpha}^n(x) Q_b(x), \quad (5)$$

for the particles with quantum numbers 0^{-+} and 1^{++} .

Let us consider the current $J_\mu^1(x)$ and charmonium hybrids H_S and H_V with $J^{PC} = 0^{+-}$ and 1^{--} as a sample case: Generalization to remaining currents is straightforward. In accordance with methodology of the sum rule analysis,

we first express the correlation function $\Pi_{\mu\nu}(p)$ in terms of the particles' physical parameters

$$\begin{aligned} \Pi_{\mu\nu}^{\text{Phys}}(p) &= \frac{\langle 0|J_\mu|H_S(p)\rangle\langle H_S(p)|J_\nu^\dagger|0\rangle}{m_S^2 - p^2} \\ &+ \frac{\langle 0|J_\mu|H_V(p,\varepsilon)\rangle\langle H_V(p,\varepsilon)|J_\nu^\dagger|0\rangle}{m_V^2 - p^2} + \dots, \end{aligned} \quad (6)$$

where m_S and m_V are the masses of the corresponding hybrids. Here, the contributions of the ground-level hybrids H_S and H_V are written down explicitly, whereas effects due to higher resonances and continuum states are denoted by the ellipses. For simplicity of the formulas, we also replace $J_\mu^1 \rightarrow J_\mu$.

The Eq. (6) is derived by inserting full set of physical states with quantum numbers of the hybrids into Eq. (1) and carrying out integration over x . The expression $\Pi_{\mu\nu}^{\text{Phys}}(p)$ can be further simplified by expressing the matrix elements in terms of the masses and current couplings of H_S and H_V

$$\langle 0|J_\mu|H_S(p)\rangle = f_S p_\mu, \quad \langle 0|J_\mu|H_V(p,\varepsilon)\rangle = m_V f_V \varepsilon_\mu, \quad (7)$$

with f_S and f_V being the current couplings of the hybrids, and ε_μ – the polarization vector of H_V .

Having substituted these matrix elements into Eq. (6), it is not difficult to find

$$\Pi_{\mu\nu}^{\text{Phys}}(p) = \frac{f_S^2}{m_S^2 - p^2} p_\mu p_\nu + \frac{m_V^2 f_V^2}{m_V^2 - p^2} \left(-g_{\mu\nu} + \frac{p_\mu p_\nu}{p^2} \right) + \dots \quad (8)$$

As is seen, the correlator $\Pi_{\mu\nu}^{\text{Phys}}(p)$ contains two Lorentz structures $g_{\mu\nu}$ and $p_\mu p_\nu$, which may be employed to derive the SRs of interest. The term proportional to $g_{\mu\nu}$ receives contribution only from the vector particle. Therefore, the relevant amplitude $\Pi_V^{\text{Phys}}(p^2)$ can be safely used to get sum rules for m_V and f_V . To isolate the contribution of the scalar state, it is convenient to multiply $\Pi_{\mu\nu}^{\text{Phys}}(p)$ by $p^\mu p^\nu / p^2$ which leads to

$$\frac{p^\mu p^\nu}{p^2} \Pi_{\mu\nu}^{\text{Phys}}(p) = \tilde{\Pi}^{\text{Phys}}(p) = -f_S^2 + \frac{m_S^2 f_S^2}{m_S^2 - p^2} + \dots \quad (9)$$

The correlation function after this operation contains only trivial Lorentz structure proportional to I . We denote corresponding invariant amplitude by $\Pi_S^{\text{Phys}}(p^2)$, and use it to obtain the SRs for parameters m_S and f_S .

The QCD side of the sum rule is determined by Eq. (1) calculated by employing the explicit expressions of the interpolating currents and replacing contractions of heavy quark fields with relevant propagators. The correlator obtained by this manner should be computed in the operator product expansion (OPE) with some accuracy. After these operations, the correlation function $\Pi_{\mu\nu}(p)$ acquires the form

$$\begin{aligned} \Pi_{\mu\nu}^{\text{OPE}}(p) &= \frac{i\varepsilon_{\mu\theta\alpha\beta}\varepsilon_{\nu\delta\alpha'\beta'}}{4} \int d^4x e^{ipx} \frac{\lambda_{ab}^n \lambda_{a'b'}^m}{4} \text{Tr} \left[S_Q^{a'a}(-x) \gamma^\theta \gamma_5 S_Q^{bb'}(x) \gamma^\delta \gamma_5 \right] \\ &\times \langle 0|g_s^2 G^{\alpha\beta}(x) G^{m\alpha'\beta'}(0)|0\rangle, \end{aligned} \quad (10)$$

where $S_Q^{ab}(x)$ is the propagator of the $Q = c$ (b) quark. In present article, we use the following expression for the propagators $S_Q^{ab}(x)$

$$\begin{aligned} S_Q^{ab}(x) &= i \int \frac{d^4k}{(2\pi)^4} e^{-ikx} \left\{ \frac{\delta_{ab}(\not{k} + m_Q)}{k^2 - m_Q^2} - \frac{g_s G_{ab}^{\alpha\beta}}{4} \frac{\sigma_{\alpha\beta}(\not{k} + m_Q) + (\not{k} + m_Q)\sigma_{\alpha\beta}}{(k^2 - m_Q^2)^2} \right. \\ &+ \frac{g_s^2 G^2}{12} \delta_{ab} m_Q \frac{k^2 + m_Q \not{k}}{(k^2 - m_Q^2)^4} + \frac{g_s^3 G^3}{48} \delta_{ab} \frac{(\not{k} + m_Q)}{(k^2 - m_Q^2)^6} \\ &\left. \times [\not{k}(k^2 - 3m_Q^2) + 2m_Q(2k^2 - m_Q^2)](\not{k} + m_Q) + \dots \right\}. \end{aligned} \quad (11)$$

Here, we have introduced the shorthand notations

$$G_{ab}^{\alpha\beta} \equiv G_n^{\alpha\beta} \lambda_{ab}^n / 2, \quad G^2 = G_{\alpha\beta}^n G_n^{\alpha\beta}, \quad G^3 = f^{nmd} G_{\alpha\beta}^n G^{m\beta\delta} G_\delta^{d\alpha}, \quad (12)$$

where f^{nmd} are structure constants of the color group $SU_c(3)$.

The $\Pi_{\mu\nu}^{\text{OPE}}(p)$ depends on two important factors: One of them is the trace term with the heavy quark propagators. The propagator $S_Q^{ab}(x)$ contains the perturbative component and nonperturbative terms proportional to $g_s^2 G^2$ and $g_s^3 G^3$ that after sandwiched between vacuum states give rise to well known gluon condensates. But there also is a term $\sim g_s G_{ab}^{\alpha\beta}$ in the propagator which having multiplied with a similar component of the second propagator generates additional two-gluon condensate: All such terms are taken into account.

Another question to be clarified here is connected with the matrix element $\langle 0 | g_s^2 G^{m\alpha\beta}(x) G^{m\alpha'\beta'}(0) | 0 \rangle$. Our treatment of this matrix element is twofold. First, we replace it by the vacuum condensate $\langle g_s^2 G^2 \rangle$ keeping the first term in the Taylor expansion at $x = 0$

$$\langle 0 | g_s^2 G^{m\alpha\beta}(x) G^{m\alpha'\beta'}(0) | 0 \rangle = \frac{\langle g_s^2 G^2 \rangle}{96} \delta^{nm} \left[g^{\alpha\beta} g^{\alpha'\beta'} - g^{\alpha\beta'} g^{\alpha'\beta} \right]. \quad (13)$$

Terms generated by this way correspond to diagrams in which the gluon interacts with the QCD vacuum. Alternatively, instead of $\langle 0 | G^{m\alpha\beta}(x) G^{m\alpha'\beta'}(0) | 0 \rangle$ we use the full gluon propagator in the x -space

$$\begin{aligned} \langle 0 | G^{m\alpha\beta}(x) G^{m\alpha'\beta'}(0) | 0 \rangle &= \frac{\delta^{nm}}{2\pi^2 x^4} \left[g^{\beta\beta'} \left(g^{\alpha\alpha'} - \frac{4x_\alpha x_{\alpha'}}{x^2} \right) \right. \\ &\quad \left. + (\beta, \beta') \leftrightarrow (\alpha, \alpha') - \beta \leftrightarrow \alpha - \beta' \leftrightarrow \alpha' \right]. \end{aligned} \quad (14)$$

Contributions obtained by this manner describe diagrams with full valence gluon propagator.

The correlator $\Pi_{\mu\nu}^{\text{OPE}}(p)$ is also a sum of terms $\sim g_{\mu\nu}$ and $\sim p_\mu p_\nu$. The amplitude $\Pi_V^{\text{OPE}}(p^2)$ that corresponds to the structure $g_{\mu\nu}$ is employed to find the parameters m_V and f_V . The amplitude $\Pi_S^{\text{OPE}}(p^2)$ extracted from the correlation function $\tilde{\Pi}^{\text{OPE}}(p) = p^\mu p^\nu \Pi_{\mu\nu}^{\text{OPE}}(p)/p^2$ is convenient to determine SRs for m_S and f_S .

Having equated the amplitudes $\Pi_S^{\text{OPE}}(p^2)$ and $\Pi_S^{\text{Phys}}(p^2)$ and carried out the Borel transformation and continuum subtraction, we find the following sum rules

$$m_S^2 = \frac{\Pi'_S(M^2, s_0)}{\Pi_S(M^2, s_0)} \quad (15)$$

and

$$f_S^2 = \frac{e^{m_S^2/M^2}}{m_S^2} \Pi_S(M^2, s_0), \quad (16)$$

where $\Pi_S(M^2, s_0)$ is the amplitude $\Pi_S^{\text{OPE}}(p^2)$ obtained after the Borel transformation and continuum subtraction procedures. Here, M^2 and s_0 are the Borel and continuum subtraction parameters, respectively. In Eq. (15), we have also introduced the short notation $\Pi'_S(M^2, s_0) = d/d(-1/M^2) \Pi_S(M^2, s_0)$.

The amplitude $\Pi_S(M^2, s_0)$ has the form

$$\Pi_S(M^2, s_0) = \int_{4m_Q^2}^{s_0} ds \rho_S^{\text{OPE}}(s) + \Pi_S(M^2), \quad (17)$$

where $\rho_S^{\text{OPE}}(s)$ is the two-point spectral density. The term $\Pi_S(M^2)$ stands for nonperturbative contributions calculated directly from $\Pi_S^{\text{OPE}}(p^2)$. Explicit expressions of the functions $\rho_S^{\text{OPE}}(s)$ and $\Pi_S(M^2)$ are rather cumbersome, therefore we do not write down them here.

In the present paper $\Pi_S(M^2, s_0)$ is computed by taking into account terms up to dimension 12. The propagator Eq. (11) contains gluon condensates of different dimensions. The dimension 4 and 6 terms proportional to condensates $\langle g_s^2 G^2 \rangle$ and $\langle g_s^3 G^3 \rangle$ appear in final expressions due to existence of relevant components in the heavy quark propagator. The terms of 8, 10 and 12 dimensions are calculated by means of the factorization hypothesis of the higher dimensional condensates. But this assumption is not precise and violates in the case of higher dimensional condensates [58]. Nevertheless, in what follows, we neglect uncertainties generated by this violation because higher dimensional contributions themselves are small.

The sum rules for m_S and f_S contain, as input parameters, gluon condensates and the mass of c quark. Below, we list their numerical values

$$\begin{aligned} \langle \alpha_s G^2 / \pi \rangle &= (0.012 \pm 0.004) \text{ GeV}^4, \quad \langle g_s^3 G^3 \rangle = (0.57 \pm 0.29) \text{ GeV}^6 \\ m_c(\mu = m_c) &= (1.27 \pm 0.02) \text{ GeV}, \quad m_b(\mu = m_b) = 4.18_{-0.02}^{+0.03} \text{ GeV}. \end{aligned} \quad (18)$$

Above we also present b quark's mass necessary for analysis of the hybrids $\bar{b}gb$ and $\bar{b}gc$. The m_c and m_b correspond to the running masses in the $\overline{\text{MS}}$ scheme at the scales $\mu = m_c$ and $\mu = m_b$ [59], respectively. The condensates $\langle\alpha_s G^2/\pi\rangle$ and $\langle g_s^3 G^3\rangle$ were extracted from analysis of hadronic processes [53, 54, 60].

Equations (15) and (16) depend on the parameters M^2 and s_0 which should be chosen to meet requirements of SR analysis. In other words, they have to ensure the dominance of the pole contribution (PC) in extracted physical quantities. Convergence of the OPE and stability of obtained results on M^2 are among important constraints as well. To keep under control these features of the SR computations, we employ

$$\text{PC} = \frac{\Pi(M^2, s_0)}{\Pi(M^2, \infty)}, \quad (19)$$

and

$$R(M^2) = \frac{\Pi^{\text{DimN}}(M^2, s_0)}{\Pi(M^2, s_0)}, \quad (20)$$

where $\Pi^{\text{DimN}}(M^2, s_0) = \sum_{N=8,10,12} \Pi^{\text{DimN}}$ is a sum of last three terms in OPE which are proportional to $\langle g_s^2 G^2 \rangle^2$, $\langle g_s^2 G^2 \rangle \langle g_s^3 G^3 \rangle$ and $\langle g_s^3 G^3 \rangle^2$, respectively.

Now, we concentrate on charmonium hybrids H_S and H_V . In Fig. 1 we plot the mass of the hybrid H_S as a function of the Borel parameter $M^2 = 3 - 10 \text{ GeV}^2$ at fixed s_0 . Our numerical computations prove that in the case of H_S the regions

$$M^2 \in [3.8, 4.8] \text{ GeV}^2, \quad s_0 \in [23, 25] \text{ GeV}^2, \quad (21)$$

meet constraints of SR analysis. Thus, at $M^2 = 4.8 \text{ GeV}^2$ and $M^2 = 3.8 \text{ GeV}^2$ on the average in s_0 the pole contribution is $\text{PC}_S \approx 0.5$ and $\text{PC}_S \approx 0.71$, respectively. At $M^2 = 3.8 \text{ GeV}^2$ the nonperturbative contribution is positive and constitutes $< 1\%$ of $\Pi_S(M^2, s_0)$. The narrowness of the window for the Borel parameter is connected with the strong restriction $\text{PC} \geq 0.5$ imposed on the pole contribution. Dependence of PC_S on the Borel parameter M^2 is plotted in Fig. 1.

The mass m_S and current coupling f_S are evaluated as mean values of these quantities over the regions Eq. (21): They are equal to

$$\begin{aligned} m_S &= (4.06 \pm 0.12 \pm 0.05 \pm 0.01) \text{ GeV}, \\ f_S &= (2.80 \pm 0.30 \pm 0.18 \pm 0.09) \times 10^{-2} \text{ GeV}^3, \end{aligned} \quad (22)$$

respectively. The results in Eq. (22) correspond to the SR predictions at the point $M^2 = 4.3 \text{ GeV}^2$ and $s_0 = 24 \text{ GeV}^2$. At these values of M^2 and s_0 the pole contribution is $\text{PC}_S \approx 0.60$, which ensures its dominance in the obtained results, and proves ground-state character of H_S in a relevant class of hybrid quarkonia.

Errors of SR computations in Eq. (22) are generated by the choices of the parameters M^2 and s_0 , ambiguities in the gluon condensate $\langle\alpha_s G^2/\pi\rangle$ and in the mass m_c , respectively. The main sources of theoretical errors in present analysis are the parameters M^2 , s_0 and the gluon condensate $\langle\alpha_s G^2/\pi\rangle$. Uncertainties of the condensate $\langle g_s^3 G^3 \rangle$ lead to corrections, which in the cases of m_S and \tilde{m}_S (see, below), for instance, are equal to $\pm 4 \times 10^{-6} \text{ GeV}$ and $< |10^{-6}| \text{ GeV}$, respectively, and therefore can be safely ignored: Throughout this work, in calculations we use for $\langle g_s^3 G^3 \rangle$ its central value. Another sources of possible errors are ones due to scale dependence of the gluon condensates and c -quark mass. But $\langle\alpha_s G^2/\pi\rangle$ is the μ -scale independent quantity, and effects of $m_c(\mu)$ and $\langle g_s^3 G^3 \rangle$ rescaling, which can be included into uncertainties of these quantities, are small and can be neglected as well. The mass m_S is shown in Fig. 2 as functions of the Borel and continuum subtraction parameters.

The spectroscopic parameters of the vector hybrid $J^{PC} = 1^{--}$ can be extracted from the sum rules Eqs. (15) and (16) after evident substitutions $\Pi_S(M^2, s_0) \rightarrow \Pi_V(M^2, s_0)$ and $(m_S, f_S) \rightarrow (m_V, f_V)$. The graphics for the mass m_V and PC_V are depicted in Fig. 3. The mass and current coupling m_V and f_V read

$$\begin{aligned} m_V &= (4.12 \pm 0.11 \pm 0.06 \pm 0.004) \text{ GeV}, \\ f_V &= (4.0 \pm 0.4 \pm 0.2 \pm 0.02) \times 10^{-2} \text{ GeV}^3, \end{aligned} \quad (23)$$

and have been extracted using the parameters

$$M^2 \in [4, 4.6] \text{ GeV}^2, \quad s_0 \in [24, 26] \text{ GeV}^2. \quad (24)$$

The quantities m_V and f_V are effectively evaluated at $M^2 = 4.3 \text{ GeV}^2$ and $s_0 = 25 \text{ GeV}^2$, where $\text{PC}_V \approx 0.58$. In Fig. 4 one can see dependence of the mass m_V on M^2 and s_0 .

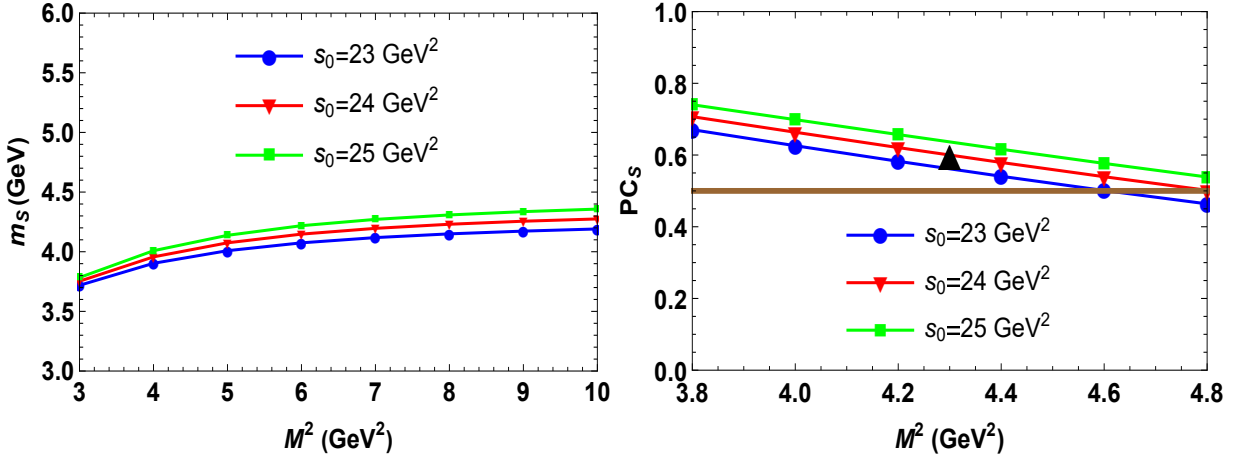


FIG. 1: Mass m_S of the scalar $J^{PC} = 0^{+-}$ charmonium hybrid as a function of the Borel parameter (left). The pole contribution PC_S vs Borel parameter M^2 at fixed s_0 for the same particle (right). The horizontal line show a region $PC = 0.5$. The triangle denote the point, where the mass m_S is extracted.

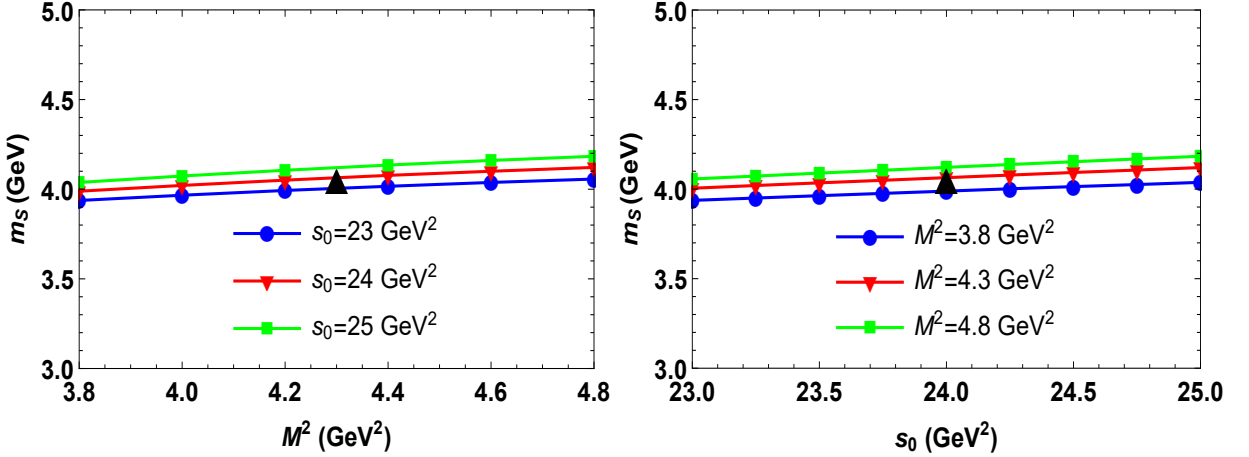


FIG. 2: Dependence of the mass m_S of the hybrid H_S on the Borel M^2 (left panel), and continuum threshold s_0 parameters (right panel). The triangles on the plots fix the position of H_S .

Parameters of the charmonium hybrids with different spin-parities J^{PC} are moved to Table I. The particles are placed in accordance with the light and heavy hybrid supermultiplet structures revealed in the MIT bag model [21, 22] and confirmed by the QCD lattice simulations [35]. The hybrids $J^{PC} = \{(0, 1, 2)^{+-}; 1^{--}\}$ composed of S -wave color-octet diquark $c\bar{c}$ and an excited gluon $J^{PC} = 1^{+-}$ form the light supermultiplet. In this paper, we have restricted ourselves by analysis of particles $J = 0, 1$, therefore this multiplet contains only three states $\{(0, 1)^{+-}; 1^{--}\}$. The heavy multiplet of the charmonium hybrids built of the P -wave diquark $c\bar{c}$ and a gluon $J^{PC} = 1^{+-}$ contains members $J^{PC} = \{(0, 1^3, 2^2, 3)^{+-}; (0, 1, 2)^{++}\}$ which in our case reduce to four states $J^{PC} = \{(0, 1)^{+-}; (0, 1)^{++}\}$.

The mass of the charmonium hybrids with spins 0 and 1 change within the limits $3.56 - 4.64$ GeV. The pseudoscalar state 0^{-+} has the mass (3.56 ± 0.10) GeV and is a lightest charmonium hybrid. This result, as well as prediction for the vector particle 1^{-+} within errors agree with ones made in Ref. [36]. The situation around the state 1^{--} is controversial and has been explained above. Our prediction $m_V = (4.12 \pm 0.13)$ GeV is compatible with $4.12 - 4.79$ GeV of Ref. [33], but is considerably larger than (3.36 ± 0.15) GeV found in Ref. [36].

In the heavy supermultiplet consisting of four hybrids the masses change from (4.06 ± 0.13) GeV for the scalar 0^{+-} to (4.53 ± 0.17) GeV for the hybrid 0^{++} . The masses of the particles 0^{++} and 1^{++} are considerably lower than ones reported in Ref. [36]. The heaviest state among considered structures is the charmonium hybrid bearing the exotic quantum numbers 0^{--} : Our result for the mass of this state (4.64 ± 0.15) GeV is 0.87 GeV smaller than prediction of [36].

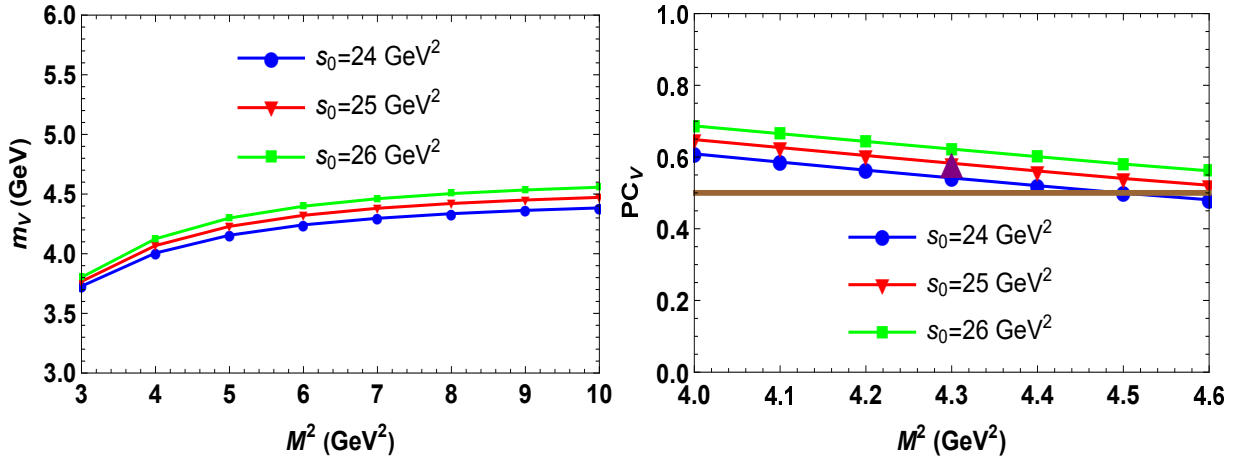


FIG. 3: The same as in Fig. 1, but for the vector charmonium hybrid $J^{PC} = 1^{--}$.

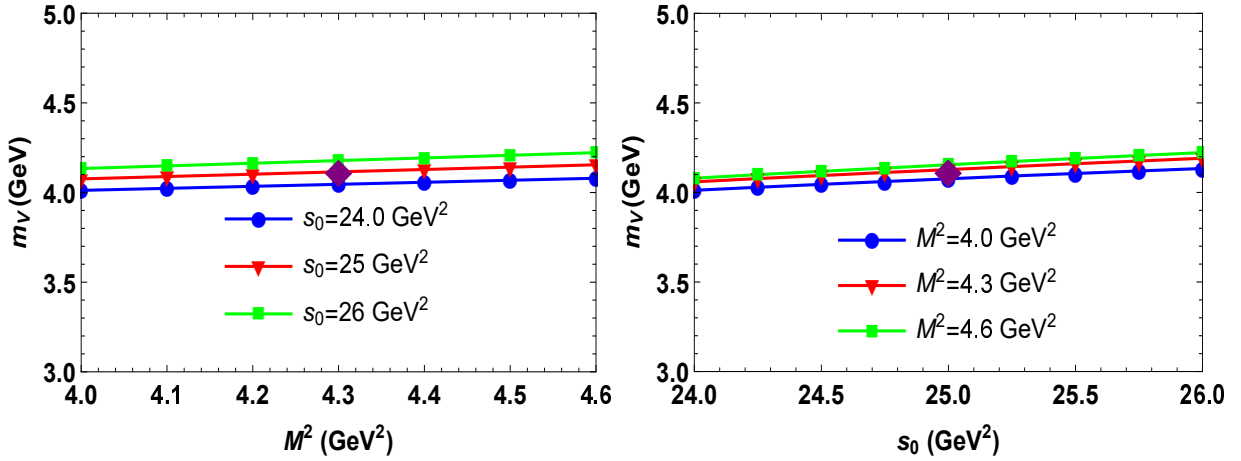


FIG. 4: The mass m_V of the vector hybrid H_V as a function of the Borel M^2 (left panel), and continuum threshold s_0 parameters (right panel). The diamonds show positions, where the mass m_V has been evaluated.

Table I also contains information on ordinary $\bar{c}c$ mesons to compare a mass hierarchy of normal and hybrid charmonia. As is seen, states 0^{-+} and 1^{--} are $\delta_c(0^{-+}) \approx 0.58$ GeV and $\delta_c(1^{--}) \approx 1$ GeV above the normal charmonia η_c and J/ψ . The hybrids 0^{++} , 1^{+-} and 1^{++} are heavier than the mesons $\chi_{c0}(1P)$, $h_c(1P)$, and $\chi_{c1}(1P)$: Their masses overshoot corresponding values approximately by $\delta_c(0^{++}) \approx 1.12$, $\delta_c(1^{+-}) \approx 0.69$, and $\delta_c(1^{++}) \approx 0.64$ GeV, respectively.

For comparison, the charmonium hybrids' parameters obtained in the context of different method are presented in Table II. Besides the sum rule predictions, we write down there results of BOEFT and QCD lattice approaches. A relatively nice agreement is observed between the present analysis and BOEFT from Ref. [51]. The lattice simulations generate considerably higher outputs [38]. Thus, the mass splitting between hybrids from the light multiplet and normal charmonia was found in Ref. [38] of around 1.2 – 1.4 GeV, whereas in the heavy supermultiplet this difference amounts to 1.1 – 1.2 GeV, which for many positions are higher than our estimates.

Information obtained for the masses of the charmonium hybrids allows us to fix their kinematically allowed two-body strong decay channels. Here, we consider this problem only qualitatively, without calculation partial widths of fixed modes. The hybrid structures can decay through open- and hidden-charm exclusive channels. Decay pattern of the hybrid mesons, their suppressed or preferable modes, model-dependent selection rules were investigated in many publications [11, 23, 27, 29, 30, 45, 52].

The all isoscalar hybrid charmonia considered here, can decay through two-body processes to standard mesons. For example, even the lightest state 0^{-+} in S -wave transforms to mesons $\eta_c f_0(500)$. The mass of the vector hybrid 1^{--}

J^{PC}	M^2 (GeV ²)	s_0 (GeV ²)	PC(%)	Mass (GeV)	$f \times 10^2$ (GeV ³)	Mass of $\bar{c}c$ meson (MeV)
0^{-+}	3.6 – 4.7	19 – 20	72 – 50	3.56(09)(04)(01)	3.8(3)(4)(07)	$\eta_c : 2983.9(4)$
1^{-+}	4 – 5	23 – 24	69 – 50	3.93(10)(07)(007)	4.60(20)(17)(11)	–
1^{--}	4 – 4.6	24 – 26	63 – 50	4.12(11)(06)(004)	4.0(4)(2)(02)	$J/\psi : 3096.900(6)$
0^{+-}	3.8 – 4.8	23 – 25	71 – 50	4.06(12)(05)(01)	2.80(30)(18)(09)	–
1^{+-}	4 – 5	25 – 27	69 – 50	4.21(15)(07)(004)	4.50(60)(04)(14)	$h_c(1P) : 3525.37(14)$
0^{++}	4 – 5	26 – 28	75 – 50	4.53(16)(07)(007)	2.50(90)(37)(05)	$\chi_{c0}(1P) : 3414.71(30)$
1^{++}	4.5 – 5.1	26 – 28	70 – 59	4.15(09)(07)(007)	5.80(50)(10)(14)	$\chi_{c1}(1P) : 3510.67(05)$
0^{--}	5 – 6.5	30 – 32	70 – 50	4.64(14)(06)(01)	4.90(50)(14)(13)	–

TABLE I: Mass and current coupling of the hybrid charmonia $\bar{c}gc$, their quantum numbers and input parameters used in calculations. We provide also the masses of the conventional $\bar{c}c$ mesons [59]. Errors of calculations and experiments are shown in a compact form, for example, 3.56(09)(04)(01) implies $3.56 \pm 0.09 \pm 0.04 \pm 0.01$.

J^{PC}	This work	SR [36]	BOEFT [51]	Lattice [38]
0^{-+}	3.56(10)	3.61(21)	3.911(54)	4.279(18)
1^{-+}	3.93(12)	3.70(21)	3.963(38)	4.310(23)
1^{--}	4.12(13)	3.36(15)	4.011(30)	4.411(17)
0^{+-}	4.06(13)	4.09(23)	4.087(61)	4.437(27)
1^{+-}	4.21(17)	4.53(23)	4.235(35)	4.665(53)
0^{++}	4.53(17)	5.34(45)	4.486(30)	4.591(46)
1^{++}	4.15(11)	5.06(44)	4.145(30)	4.518(35)
0^{--}	4.64(15)	5.51(50)	–	–

TABLE II: Predictions for the masses (in GeV units) of the hybrid charmonia $\bar{c}gc$ obtained in different articles.

makes the S -wave hidden-charm channel

$$H_V \rightarrow J/\psi f_0(500), \quad (25)$$

a possible process for this particle. The open-charm P -wave decays

$$H_V \rightarrow D\bar{D}, D_0\bar{D}_0, D_s\bar{D}_s \quad (26)$$

are among kinematically allowed modes of H_V as well.

The hybrid bottomonia $\bar{b}gb$ can be studied in accordance with the scheme outlined above. The differences here are connected with the mass of b -quark, and a necessity to choose new parameters M^2 and s_0 in such a way that to satisfy requirements of SR calculations. Our studies demonstrate that for the bottomonia counterparts of scalar and vector charmonium hybrids, i.e., for states 0^{+-} and 1^{--} the Borel and continuum threshold parameters have to be fixed in the following limits: for the scalar particle

$$M^2 \in [12, 13.5] \text{ GeV}^2, \quad s_0 \in [124, 126] \text{ GeV}^2 \quad (27)$$

and for the vector state

$$M^2 \in [12, 14] \text{ GeV}^2, \quad s_0 \in [120, 125] \text{ GeV}^2. \quad (28)$$

The mass and current coupling of the structures 0^{+-} and 1^{--} are equal to

$$\begin{aligned} \tilde{m}_S &= (10.12 \pm 0.06 \pm 0.06 \pm 0.01) \text{ GeV}, \\ \tilde{f}_S &= (4.6 \pm 0.3 \pm 0.7 \pm 0.2) \times 10^{-2} \text{ GeV}^3, \end{aligned} \quad (29)$$

and

$$\begin{aligned} \tilde{m}_V &= (10.41 \pm 0.18 \pm 0.08 \pm 0.012) \text{ GeV}, \\ \tilde{f}_V &= (12.0 \pm 3.0 \pm 0.6 \pm 0.4) \times 10^{-2} \text{ GeV}^3, \end{aligned} \quad (30)$$

J^{PC}	M^2 (GeV ²)	s_0 (GeV ²)	PC(%)	Mass (GeV)	$f \times 10^2$ (GeV ³)	Mass of $\bar{b}b$ meson (MeV)
0^{-+}	11 – 13	110 – 120	67 – 50	9.68(20)(07)(012)	9.2(1.9)(0.28)(0.27)	$\eta_b : 9398.7(2.0)$
1^{-+}	12 – 13	115 – 120	60 – 51	9.85(11)(08)(01)	8.9(1.0)(0.13)(0.34)	–
1^{--}	12 – 14	120 – 125	72 – 51	10.41(18)(08)(012)	12.0(3.0)(0.6)(0.4)	$\Upsilon(1S) : 9460.40(09)(04)$
0^{+-}	12 – 13.5	124 – 126	66 – 50	10.12(06)(06)(01)	4.6(3)(7)(2)	–
1^{+-}	13.5 – 14.5	130 – 132	56 – 50	10.46(06)(07)(01)	11.60(60)(13)(42)	$h_b(1P) : 9899.3(8)$
0^{++}	13.5 – 15	125 – 130	60 – 50	10.57(08)(08)(02)	19.3(1.6)(0.2)(0.5)	$\chi_{b0}(1P) : 9859.44(42)(31)$
1^{++}	12.5 – 14.5	128 – 130	65 – 51	10.55(10)(08)(02)	13.4(1.0)(0.07)(0.44)	$\chi_{b1}(1P) : 9892.78(26)(31)$
0^{--}	12 – 14	130 – 135	76 – 50	10.51(11)(06)(02)	3.90(30)(09)(18)	–

TABLE III: The same as in Table I, but for the bottomonia hybrids $\bar{b}gb$. The masses of the mesons $\bar{b}b$ are borrowed from Ref. [59].

J^{PC}	This work	SR [36]	BOEFT [51]	Lattice [44]
0^{-+}	9.68(21)	9.68(29)	10.682(5)	10.926(18)
1^{-+}	9.85(14)	9.79(22)	10.686(4)	10.935(18)
1^{--}	10.41(20)	9.70(12)	10.6902(30)	10.952(24)
0^{+-}	10.12(09)	10.17(22)	10.756(5)	10.935(41)
1^{+-}	10.46(09)	10.70(53)	10.759(4)	11.062(35)
0^{++}	10.57(12)	11.20(48)	11.012(3)	–
1^{++}	10.55(13)	11.09(60)	10.761(3)	10.921(55)
0^{--}	10.51(13)	11.48(75)	–	–

TABLE IV: Masses (in GeV units) of the bottomonium hybrids $\bar{b}gb$ extracted in the framework of SR, BOEFT and lattice methods.

respectively.

Other $\bar{b}gb$ states are investigated with similar manner: Results obtained for the hybrid bottomonia are collected in Table III and occupy the mass range of 9.68 – 10.57 GeV. The particles 0^{-+} and 1^{-+} from the light supermultiplet have the masses (9.68 ± 0.21) GeV and (9.85 ± 0.14) GeV, which coincide with or are very close to ones from Ref. [36]. But they are considerably lower than predictions of QCD lattice and BOEFT analyses. In these approaches masses of the hybrids 0^{-+} and 1^{-+} were found equal to (10.926 ± 0.018) GeV and (10.935 ± 0.018) GeV [44], and (10.682 ± 0.005) GeV and (10.686 ± 0.004) GeV [51], respectively. In our analysis, the vector hybrid 1^{--} has the mass (10.41 ± 0.20) GeV which agrees with the result of Ref. [33]. But it is significantly larger than (9.70 ± 0.12) GeV of Ref. [36], and smaller the lattice and BOEFT predictions.

For bottomonium hybrids from the light supermultiplet the lattice simulations predict the spin-average mass $\simeq 10.938$ GeV [44]. For particles from the heavy supermultiplet this parameter equals to 10.872 GeV. The Born-Oppenheimer approximation generates the following average masses [51]: The 10.686 GeV and 10.822 GeV for the light and heavy supermultiplets, respectively. One of features of the lattice and BOEFT spectra is a mass degeneration between the light and heavy supermultiplets. Comparing these data with our results from Table III and corresponding spin-averages 9.98 GeV and 10.425 GeV in the multiplets, we note approximately 1 GeV and 0.4 GeV mass gaps between SR and lattice predictions. In other words, for the hybrid bottomonia the sum rule calculations give an increasing mass spectrum (see Table IV).

The two-body strong decay channels of the $\bar{b}gb$ hybrids is analyzed based on our estimations. The masses of the hybrids 0^{-+} and 1^{-+} are below thresholds for production of open- and hidden-bottom two-meson pairs. This conclusion is correct even for upper limits of their masses. The vector hybrid 1^{--} can easily decay in S -wave to mesons $\Upsilon(1S)f_0(500)$. The scalar particle 0^{+-} has the mass (10.12 ± 0.09) GeV and decays in P -wave to a pair $\Upsilon(1S)f_0(500)$. Kinematically allowed two-body decay channels of the remaining heavy charmonium and bottomonium hybrids can be found in Ref. [37] by taking into account the masses of these particles found in the present work.

J^{PC}	M^2 (GeV ²)	s_0 (GeV ²)	PC(%)	Mass (GeV)	$f \times 10^2$ (GeV ³)	Mass of $\bar{b}c$ meson (MeV)
$0^{-(+)}$	7 – 8	55 – 57	69 – 51	6.55(08)(06)(009)(007)	4.9(4)(3)(09)(04)	$B_c(1S) : 6274.47(27)(17)$
$1^{-(+)}$	6.8 – 7.8	55 – 60	62 – 50	6.63(14)(07)(007)(007)	4.50(70)(18)(09)(04)	–
$1^{-(-)}$	7 – 8.3	62 – 65	71 – 55	7.01(13)(08)(006)(002)	4.80(60)(05)(11)(07)	$B_c^*[B_c(1^3S_1)] : 6338$
$0^{+(-)}$	8.5 – 9.4	58 – 60	61 – 53	6.93(07)(05)(006)(006)	2.80(20)(19)(06)(05)	–
$1^{+(-)}$	7.6 – 8.6	65 – 67	61 – 50	7.17(09)(07)(005)(004)	5.70(50)(08)(13)(07)	$B_c(1^1P_1) : 6750$
$0^{+(+)}$	8 – 10	65 – 67	70 – 50	7.03(12)(08)(008)(005)	8.1(8)(2)(1)(07)	$B(1^3P_0) : 6706$
$1^{+(+)}$	8 – 9.5	66 – 67	65 – 50	7.12(09)(08)(007)(004)	7.40(50)(06)(14)(08)	$B(1^3P_1) : 6741$
$0^{-(-)}$	7.8 – 8.8	66 – 67	62 – 50	7.19(06)(06)(007)(006)	4.00(20)(13)(08)(06)	–

TABLE V: The parameters of the bottom-charm hybrid mesons $\bar{b}gc$. The errors are generated by ambiguities in (M^2, s_0) , $\langle\alpha_s G^2/\pi\rangle$, m_b , and m_c , respectively. The last column contains masses of the mesons $\bar{b}c$. As the mass of the meson $B_c^+(1S)$, we use its experimental value [59]. The masses of the remaining $\bar{b}c$ mesons are theoretical predictions obtained by means of the relativized quark model [61].

III. THE HEAVY HYBRID MESONS $\bar{b}gc$

In this section, we consider the heavy hybrid mesons $\bar{b}gc$ and evaluate masses of these structures with the spin-parities $J^{\text{P}} = 0^+, 0^-, 1^+, \text{ and } 1^-$. Relevant currents can easily be obtained from Eqs. (2), (3), (4) and (5). It is clear that charged hybrids $\bar{b}gc$ can not be classified by C-parity. But to distinguish particles explored by means of different currents, we keep formally in parenthesis the C-parity of original currents. The current that corresponds to the hybrids $J^{\text{P}} = 0^{+(-)}$ and $1^{-(-)}$ is

$$\tilde{J}_\mu^1(x) = g_s \bar{b}_a(x) \gamma^\alpha \gamma_5 \frac{\lambda_{ab}^n}{2} \tilde{G}_{\mu\alpha}^n(x) c_b(x). \quad (31)$$

The scalar and vector particles with $J^{\text{P}} = 0^{+(+)}$ and $1^{-(-)}$ can be investigated using the current

$$\tilde{J}_\mu^2(x) = g_s \bar{b}_a(x) \gamma^\alpha \frac{\lambda_{ab}^n}{2} G_{\mu\alpha}^n(x) c_b(x). \quad (32)$$

The particles $0^{-(-)}$ and $1^{+(-)}$ are described by the current

$$\tilde{J}_\mu^3(x) = g_s \bar{b}_a(x) \gamma^\alpha \gamma_5 \frac{\lambda_{ab}^n}{2} G_{\mu\alpha}^n(x) c_b(x). \quad (33)$$

The current

$$\tilde{J}_\mu^4(x) = g_s \bar{b}_a(x) \gamma^\alpha \frac{\lambda_{ab}^n}{2} \tilde{G}_{\mu\alpha}^n(x) c_b(x), \quad (34)$$

corresponds to the pseudoscalar and axial-vector hybrids $J^{\text{P}} = 0^{-(-)}$ and $1^{+(-)}$.

The correlation functions $\tilde{\Pi}_{\mu\nu}(p)$ to be studied in these cases are given by Eq. (1) after replacement $J_\mu(x) \rightarrow \tilde{J}_\mu(x)$. Treatment of the relevant correlators does not differ considerably from the analysis presented in the previous section. Differences appear only in the QCD sides of SRs. For instance, in the case of the current $\tilde{J}_\mu^1(x)$ the correlator $\tilde{\Pi}_{\mu\nu}^{\text{OPE}}(p)$ is determined by the formula

$$\begin{aligned} \tilde{\Pi}_{\mu\nu}^{\text{OPE}}(p) &= \frac{i\varepsilon_{\mu\theta\alpha\beta}\varepsilon_{\nu\delta\alpha'\beta'}}{4} \int d^4x e^{ipx} \frac{\lambda_{ab}^n \lambda_{a'b'}^m}{4} \text{Tr} \left[S_b^{a'a}(-x) \gamma^\theta \gamma_5 S_c^{bb'}(x) \gamma^\delta \gamma_5 \right] \\ &\times \langle 0 | g_s^2 G^{m\alpha\beta}(x) G^{m\alpha'\beta'}(0) | 0 \rangle. \end{aligned} \quad (35)$$

Parameters of the bottom-charm hybrids obtained using these interpolating currents are presented in Table V. As samples, in Fig. 5 we show masses of the pseudoscalar and vector particles $0^{-(-)}$ and $1^{+(-)}$.

The masses of the hybrid mesons $\bar{b}gc$ change in the interval 6.55 – 7.19 GeV. The average masses of hybrids conditionally belonging to the light multiplet 6.73 GeV is close to 6.9 GeV from Ref. [37] and only 0.4 GeV higher than a mass average of two mesons B_c and B_c^* . But our predictions for the particles from the heavy multiplet are considerably smaller than results presented there. The spectrum of the hybrid mesons $\bar{b}gc$ evaluated in the present work is very smooth relative to predictions of Ref. [37], where the masses vary inside limits 6.83 – 8.48 GeV.

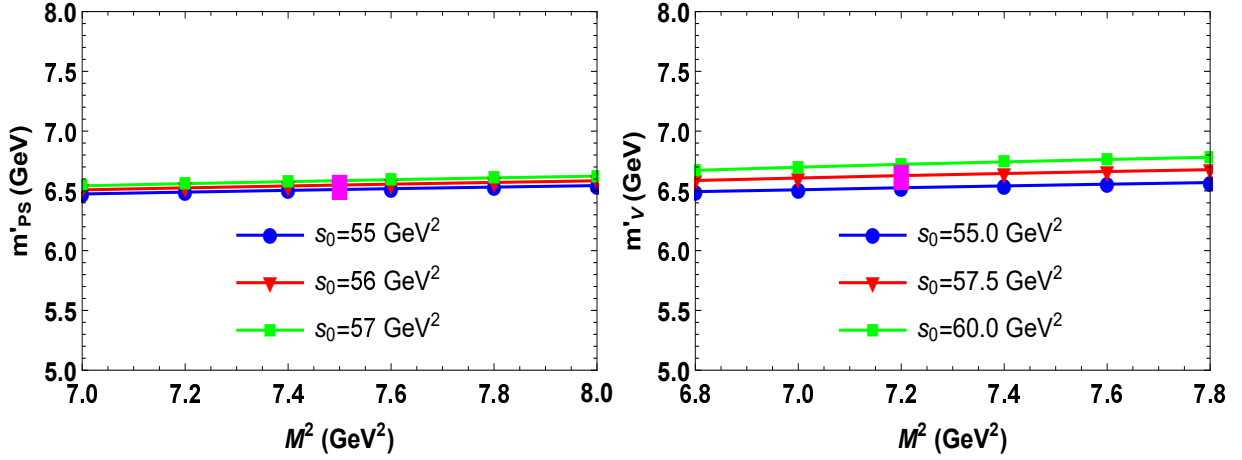


FIG. 5: Masses of the pseudoscalar $0^{-(+)}$ (left panel) and vector $1^{-(+)}$ (right panel) hybrids $\bar{b}gc$ as functions of the Borel parameter. The rectangles on plots note the hybrid masses.

The possible two-body strong decay modes of the hybrids $\bar{b}gc$ are determined by thresholds for production of meson pairs with appropriate quantum numbers. The hybrids $0^{-(+)}$ and $1^{-(+)}$ are light particles, and seem are stable against strong two-body decays to standard heavy mesons. The next state in the table $1^{-(-)}$ has allowed channels $1^{-(-)} \rightarrow B_c^{*+} f_0(500)$ and $B_c^+ \eta$ which are its S - and P -wave decay modes, respectively. The hybrid $0^{+(-)}$ transforms to the meson pairs $B_c^+ \eta$ and $B_c^{*+} f_0(500)$. The decay channels of the particles $1^{+(-)}$ and $1^{+(+)}$ are processes $1^{+(-)} \rightarrow B_c^{*+} \eta$, $B_c^+ f_0(500)$, $B_c^+ \omega(782)$ and $1^{+(+)} \rightarrow B_c^{*+} f_0(500)$. The particles $0^{+(+)}$ and $0^{-(-)}$ can decay through the modes $0^{+(+)} \rightarrow B_c^+ \eta$, $B^+ D^0$ and $0^{-(-)} \rightarrow B_c^+ f_0(500)$, $B_c^{*+} \eta$.

IV. CONCLUSIONS

In this article, we have investigated the scalar, pseudoscalar, vector and axial-vector charmonium and bottomonium hybrids with positive and negative C -parities in the context of QCD two-point sum rule approach and extracted their masses and current couplings. We have also studied the hybrid mesons $\bar{b}gc$ with the spin-parities $J^P = 0^+$, 0^- , 1^+ , and 1^- .

In our calculations, we have taken into account nonperturbative terms up to dimension 12. The higher dimensional terms despite the fact that are numerically small may be important to improve the stability of SR calculations. We also imposed the strong restriction on the pole contribution $PC \geq 0.5$ which is necessary to extract reliable predictions for physical quantities under consideration.

Results obtained for the masses of these structures were used to reveal their possible two-body strong decay channels. It has been demonstrated that all charmonium hybrids are unstable against strong decays. The $\bar{c}gc$ hybrid 1^{--} which was predicted to be stable [36], in our case has the mass $m_V = (4.12 \pm 0.11)$ GeV and decays through open- and hidden-charm channels to different meson pairs.

In the class of the hybrid bottomonia only the particles 0^{--} and 1^{--} with the masses (9.68 ± 0.21) GeV and (9.85 ± 0.14) GeV are strong-interaction stable structures, because their masses are below thresholds for production of open- and hidden-bottom meson pairs. The exotic mesons $\bar{b}gc$ with quantum numbers $0^{-(+)}$ and $1^{-(+)}$ are also stable against strong two-body decays to standard heavy mesons.

Comparing our results with predictions of Refs. [36, 37], we see that there are differences between them. The discrepancies are essential for hybrids from the heavy multiplets, although large uncertainties in extracted masses create overlapping regions for some of particles. In our view, such deviations are presumably connected with the requirement $PC \geq 0.5$ imposed on the pole contributions in the present analysis.

A nice agreement is achieved with BOEFT results for the charmonium hybrids. In the case of $\bar{b}gb$ mesons this effective field theory leads to predictions, especially for the light multiplet, which are higher than ours. The largest outputs for parameters of the heavy hybrids are generated by the lattice simulations.

The sum rule analysis performed in the present work and comparisons with results of alternative methods are important to shed light on properties of the exotic hybrid mesons. The predictions obtained for the spectroscopic parameters of the hybrids can be used in investigations of strong and electroweak decays of these particles as well as to study their interactions with other hadrons.

ACKNOWLEDGMENTS

H. Sundu is thankful to Scientific and Technological Research Council of Türkiye (TUBITAK) for the financial support provided under the Grant No. 123F197. K. Azizi is thankful to Iran National Science Foundation (INSF) for the partial financial support provided under the elites Grant No. 4025036.

-
- [1] R. Aaij *et al.* (LHCb Collaboration), Sci. Bull. **65**, 1983 (2020).
 - [2] E. Bouhova-Thacker (ATLAS Collaboration), PoS **ICHEP2022**, 806 (2022).
 - [3] A. Hayrapetyan, *et al.* (CMS Collaboration) arXiv:2306.07164 [hep-ex].
 - [4] R. Aaij *et al.* (LHCb Collaboration), Phys. Rev. Lett. **115**, 072001 (2015).
 - [5] R. Aaij *et al.* (LHCb Collaboration), Phys. Rev. Lett. **122**, 222001 (2019).
 - [6] R. Aaij *et al.* (LHCb Collaboration), Sci. Bull. **66**, 1278 (2021).
 - [7] M. Ablikim *et al.* (BESIII Collaboration), Phys. Rev. Lett. **129**, 192002 (2022)[E.**130**, 159901 (2023)].
 - [8] H. X. Chen, N. Su, and S. L. Zhu, Chin. Phys. Lett. **39**, 051201 (2022).
 - [9] L. Qiu, and Q. Zhao, Chin. Phys. Lett. **46**, 051001 (2022).
 - [10] V. Shastri, C. S. Fischer, and F. Giacosa, Phys. Lett. B **834**, 137478 (2022).
 - [11] E. Kou, and O. Pene, Phys. Lett. B **631**, 164 (2005).
 - [12] S. L. Olsen, T. Skwarnicki, and D. Zieminska, Rev. Mod. Phys. **90**, 015003 (2018).
 - [13] N. Brambilla, W. K. Lai, A. Mohapatra, and A. Vairo, Phys. Rev. D **107**, 054034 (2023).
 - [14] A. Engler, H. E. Fisk, R. w. Kramer, C. M. Meltzer, and J. B. Westgard, Phys. Rev. Lett. **15**, 224 (1965).
 - [15] M. Niiyama *et al.*, Phys. Rev. C **78**, 035202 (2008).
 - [16] G. Agakishiev *et al.* (HADES Collaboration), Phys. Rev. C **87**, 025201 (2013).
 - [17] K. Moriya *et al.* (CLAS Collaboration), Phys. Rev. C **88**, 045201 (2013) Addendum:[Phys. Rev. C **88**, 049902 (2013)].
 - [18] R. L. Jaffe and K. Johnson, Phys. Lett. B **60**, 201 (1976).
 - [19] D. Horn, and L. Mandula, Phys. Rev. D **17**, 898 (1978).
 - [20] M. Tanimoto, Phys. Rev. D **27**, 2648 (1983).
 - [21] T. Barnes, F. E. Close, and F. de Viron, Nucl. Phys. B **224**, 241 (1983).
 - [22] M. S. Chanowitz, and S. R. Sharpe, Nucl. Phys. B **222**, 211 (1983).
 - [23] N. Isgur, R. Kokoski, and J. Paton Phys. Rev. Lett. **54**, 869 (1985).
 - [24] F. de Viron, and J. Govaerts, Phys. Rev. Lett. **53**, 2207 (1984).
 - [25] J. Govaerts, L. J. Reinders, H. R. Rubinstein, and J. Weyers, Nucl. Phys. B **258**, 215 (1985).
 - [26] J. Govaerts, L. J. Reinders, and J. Weyers, Nucl. Phys. B **262**, 575 (1985).
 - [27] F. E. Close, and P. R. Page, Nucl. Phys. B **443**, 233 (1995).
 - [28] F. E. Close, and P. R. Page, Phys. Rev. D **52**, 1706 (1995).
 - [29] P. R. Page, Phys. Lett. B **402**, 183 (1997).
 - [30] P. R. Page, E. S. Swanson, and A. P. Szczepaniak, Phys. Rev. D **59**, 034016 (1999).
 - [31] S. L. Zhu, Phys. Rev. D **60**, 014008 (1999).
 - [32] S. Narison, Phys. Lett. B **675**, 319 (2009).
 - [33] C. F. Diao, L. Tang, G. Hao, and X. Q. Li, J. Phys. G **39**, 015005 (2012).
 - [34] D. Harnett, R. T. Kleiv, T. G. Steele, and H. y. Jin, J. Phys. G **39**, 125003 (2012).
 - [35] L. Liu *et al.* (Hadron Spectrum Collaboration), JHEP **07**, 126 (2012).
 - [36] W. Chen, R. T. Kleiv, T. G. Steele, B. Bulthuis, D. Harnett, T. Ho, T. Richards, and S. L. Zhu, JHEP **09**, 019 (2013).
 - [37] W. Chen, T. G. Steele, and S. L. Zhu, J. Phys. G **41**, 025003 (2014).
 - [38] G. K. C. Cheung *et al.* (Hadron Spectrum Collaboration), JHEP **12**, 089 (2016).
 - [39] K. Azizi, B. Barsbay, and H. Sundu, Eur. Phys. J. Plus **133**, 121 (2018).
 - [40] Z. R. Huang, H. Y. Jin, and Z. F. Zhang JHEP **04**, 004 (2015).
 - [41] A. Palameta, D. Harnett, and T. G. Steele, Phys. Rev. D **98**, 074014 (2018).
 - [42] T. Miyamoto and S. Yasui, Phys. Rev. D **99**, 094015 (2019).
 - [43] N. Brambilla, W. K. Lai, J. Segovia, J. Tarrus Castella, and A. Vairo, Phys. Rev. D **99**, 014017 (2019)[Erratum: Phys. Rev. D **101**, 099902 (2020)].
 - [44] S. M. Ryan, and D. J. Wilson, JHEP **02**, 214 (2021).
 - [45] J. Tarrús Castellà and E. Passemar, Phys. Rev. D **104**, 034019 (2021).
 - [46] A. J. Woss *et al.* (Hadron Spectrum Collaboration), Phys. Rev. D **103**, 054502 (2021).
 - [47] B. Barsbay, K. Azizi, and H. Sundu, Eur. Phys. J. C **82**, 1138 (2022).
 - [48] B. Barsbay, K. Azizi, and H. Sundu, arXiv:2402.19006 [hep-ph].
 - [49] C. M. Tang, Y. C. Zhao, and L. Tang, Phys. Rev. D **105**, 114004 (2022).
 - [50] F. Chen, X. Jiang, Y. Chen, M. Gong, Z. Liu, C. Shi, and W. Sun, Phys. Rev. D **107**, 054511 (2023).
 - [51] J. Soto, and S. T. Valls, Phys. Rev. D **108**, 014025 (2023).
 - [52] R. Bruschini, Phys. Rev. D **109**, L031501 (2024).
 - [53] M. A. Shifman, A. I. Vainshtein and V. I. Zakharov, Nucl. Phys. B **147**, 385 (1979).

- [54] M. A. Shifman, A. I. Vainshtein and V. I. Zakharov, Nucl. Phys. B **147**, 448 (1979).
- [55] M. Nielsen, F. S. Navarra, and S. H. Lee, Phys. Rept. **497**, 41 (2010).
- [56] R. M. Albuquerque, J. M. Dias, K. P. Khemchandani, A. Martinez Torres, F. S. Navarra, M. Nielsen and C. M. Zanetti, J. Phys. G **46**, 093002 (2019).
- [57] S. S. Agaev, K. Azizi, and H. Sundu, Turk. J. Phys. **44**, 95 (2020).
- [58] B. L. Ioffe, Prog. Part. Nucl. Phys. **56**, 232 (2006).
- [59] R. L. Workman *et al.* [Particle Data Group], Prog. Theor. Exp. Phys. **2022**, 083C01 (2022).
- [60] S. Narison, Nucl. Part. Phys. Proc. **270-272**, 143 (2016).
- [61] S. Godfrey, Phys. Rev. D **70**, 054017 (2004).